Applied Mathematics Letters 154 (2024) 109103

Contents lists available at ScienceDirect

Applied Mathematics Letters

journal homepage: www.elsevier.com/locate/aml

Regular article

Analysis of a nonlocal diffusion model with a weakly singular kernel

Jinhong Jia [a], Zhiwei Yang [b], Hong Wang [c,*]

[a] School of Mathematics and Statistics, Shandong Normal University, Jinan, Shandong 250358, China
[b] Research Institute of Intelligent Complex Systems, School of Mathematical Sciences, Fudan University, Shanghai, 200433, China
[c] Department of Mathematics, University of South Carolina, Columbia, SC 29208, USA

ARTICLE INFO

Keywords:
Nonlocal diffusion model
Weakly singular kernel
Fourier transform

ABSTRACT

We establish that *for any fixed horizon* $\delta > 0$, the solution of a nonlocal diffusion model with a weakly singular kernel p_δ converges asymptotically to the solution of the corresponding Fickian diffusion equation. The diffusion tensor of the Fickian equation is determined by half of the covariance matrix, with p_δ serving as the probability density function. Numerical experiments are performed to validate our findings. Additionally, we observe that the mean square displacement of the nonlocal diffusion model exhibits a linear relationship with respect to time t.

1. Introduction

Nonlocal models, exemplified by the nonlocal diffusion model [1–3] and the fractional diffusion equation [4–6], offer a powerful framework for describing (anomalously) diffusive transport in the natural world. They overcome limitations inherent in classical integer-order diffusion equations, providing a more comprehensive representation of these phenomena. The versatility of nonlocal models allows them to tailor their form to the unique characteristics of the phenomena at hand. In this paper, we focus on the nonlocal diffusion model

$$\begin{gathered}\frac{\partial u}{\partial t}(t,\boldsymbol{x}) = \int_{B_\delta(\boldsymbol{x})} p_\delta(|\boldsymbol{x}-\boldsymbol{y}|)\big(u(t,\boldsymbol{y}) - u(t,\boldsymbol{x})\big)\,d\boldsymbol{y} \quad (t,\boldsymbol{x}) \in \mathbb{R}^+ \times \mathbb{R}^d, \\ u(0,\boldsymbol{x}) = u_0(\boldsymbol{x}), \quad \boldsymbol{x} \in \mathbb{R}^d.\end{gathered} \tag{1}$$

Here d is the dimension of the space. The horizon $\delta > 0$ defines the extent of nonlocal interactions. The neighborhood $B_\delta(\boldsymbol{x}) \subset \mathbb{R}^d$ represents the closed ball in the l_γ norm, denoted by $|\cdot|\gamma$ with $1 \le \gamma \le \infty$ [7]. This ball has a radius of δ and is centered at the point $\boldsymbol{x}$. Additionally, the kernel $p_\delta(|\boldsymbol{x}|)$ is assumed to be a nonnegative function with compact support within $B_\delta(\boldsymbol{0})$.

The investigation into the asymptotic behavior of the nonlocal diffusion model and its connection with the integer-order diffusion equation stands as a central theme in nonlocal diffusion model research. Previous studies in the literature have primarily concentrated on understanding the behavior of the nonlocal diffusion model as δ tends to 0. Under appropriate assumptions regarding the kernel p_δ, findings in [2] illustrate that as $\delta \to 0$, the nonlocal effect diminishes. Consequently, the nonlocal diffusion model converges to the classical local differential equation in the local limit.

In this paper, we establish that *for any fixed* $\delta > 0$, the solution of the nonlocal diffusion model (1) with a weakly singular kernel p_δ converges asymptotically to the solution of the corresponding Fickian diffusion equation. The diffusion tensor of the Fickian equation is determined by half of the covariance matrix, with p_δ serving as the probability density function. The detailed analysis is presented in Section 2. In Section 3, we conduct numerical experiments to validate our findings. Additionally, we observe that the mean square displacement of the nonlocal diffusion model exhibits a linear relationship with respect to time t.

* Corresponding author.
E-mail addresses: jhjia@sdnu.edu.cn (J. Jia), zhiweiyang@fudan.edu.cn (Z. Yang), hwang@math.sc.edu (H. Wang).

https://doi.org/10.1016/j.aml.2024.109103
Received 31 January 2024; Received in revised form 3 April 2024; Accepted 3 April 2024
Available online 9 April 2024
0893-9659/

2. Asymptotic analysis

The nonlocal diffusion model, denoted by (1), comprises a nonlocal spatial term alongside a first-order temporal differential operator known for its exponentially decaying local behavior over time. Our current investigation aims to elucidate whether the formally nonlocal spatial component within (1) demonstrates local or nonlocal behavior in space asymptotically. This endeavor essentially boils down to discerning the tail behavior of $u(t,\boldsymbol{x})$ as $\boldsymbol{x} \to \pm\infty$. This task is tantamount to determining the behavior of the Fourier transform of the probability density function (i.e., the normalized unknown variable u) in the phase plane as $\boldsymbol{k} \to \boldsymbol{0}$. To facilitate this analysis, we introduce the Fourier transform for the function $\lambda(\boldsymbol{x})$ [8,9]

$$\hat{\lambda}(\boldsymbol{k}) := \mathcal{F}[\lambda](\boldsymbol{k}) := \int_{\mathbb{R}^d} \lambda(\boldsymbol{x}) e^{-\mathrm{i}\boldsymbol{k}\cdot\boldsymbol{x}} d\boldsymbol{x}.$$

We expand the analysis in [9] by applying it to the nonlocal diffusion model (1). Let $\boldsymbol{X} := [X_1, X_2, \dots, X_d]^\top$ be the random vector. We are now in the position to proving the main result of this paper for the nonlocal diffusion model (1) in the following theorem.

Theorem 2.1. *Assume that the kernel $p_\delta(|\boldsymbol{x}|)$ in the nonlocal diffusion model (1) is weakly singular, i.e.,*

$$\int_{B_\delta(\boldsymbol{0})} p_\delta(|\boldsymbol{x}|) d\boldsymbol{x} < \infty. \tag{2}$$

Then for any fixed $\delta > 0$, the nonlocal model (1) demonstrates asymptotic equivalence to the d-dimensional Fickian diffusion equation

$$\begin{aligned} &\frac{\partial u}{\partial t}(t,\boldsymbol{x}) = \nabla \cdot (\mathbf{K}\nabla u(t,\boldsymbol{x})) \quad && (t,\boldsymbol{x}) \in \mathbb{R}^+ \times \mathbb{R}^d, \\ &u(0,\boldsymbol{x}) = u_0(\boldsymbol{x}) && \boldsymbol{x} \in \mathbb{R}^d. \end{aligned} \tag{3}$$

Here the diffusion tensor $\boldsymbol{K}$ is defined by

$$\begin{aligned} &\mathbf{K} := \frac{1}{2} Cov(\boldsymbol{X}) := \frac{1}{2} \begin{bmatrix} \mathbb{E}(X_1^2) & \dots & \mathbb{E}(X_1 X_d) \\ \vdots & \dots & \vdots \\ \mathbb{E}(X_1 X_d) & \dots & \mathbb{E}(X_d^2) \end{bmatrix}, \\ &\mathbb{E}(X_i X_j) := \int_{B_\delta(\boldsymbol{0})} x_i x_j p_\delta(\boldsymbol{x}) d\boldsymbol{x}, \qquad 1 \le i,j \le d. \end{aligned} \tag{4}$$

Proof. We set $\boldsymbol{z} := \boldsymbol{x} - \boldsymbol{y}$, then the right-hand side of (1) can be rewritten as

$$\begin{aligned} G(t,\boldsymbol{x}) &= \int_{B_\delta(\boldsymbol{x})} p_\delta(|\boldsymbol{x}-\boldsymbol{y}|)\big(u(t,\boldsymbol{y}) - u(t,\boldsymbol{x})\big) d\boldsymbol{y} \\ &= \int_{B_\delta(\boldsymbol{0})} p_\delta(|\boldsymbol{z}|)\big(u(t,\boldsymbol{x}-\boldsymbol{z}) - u(t,\boldsymbol{x})\big) d\boldsymbol{z} \\ &= p_\delta(|\boldsymbol{x}|) * u(t,\boldsymbol{x}) - \Big(\int_{B_\delta(\boldsymbol{0})} p_\delta(|\boldsymbol{z}|) d\boldsymbol{z}\Big) u(t,\boldsymbol{x}). \end{aligned}$$

Take the Fourier transform of G to obtain

$$\hat{G}(t,\boldsymbol{k}) = \hat{p}_\delta(\boldsymbol{k})\hat{u}(t,\boldsymbol{k}) - \Big(\int_{B_\delta(\boldsymbol{0})} p_\delta(|\boldsymbol{z}|) d\boldsymbol{z}\Big)\hat{u}(t,\boldsymbol{k}). \tag{5}$$

We evaluate the Fourier transform $\hat{p}_\delta(\boldsymbol{k})$ of the kernel $p_\delta(\boldsymbol{k})$ as follows

$$\begin{aligned} \hat{p}_\delta(\boldsymbol{k}) &= \int_{\mathbb{R}^d} e^{-\mathrm{i}\boldsymbol{k}\cdot\boldsymbol{x}} p_\delta(|\boldsymbol{x}|) d\boldsymbol{x} \\ &= \int_{B_\delta(\boldsymbol{0})} \Big(1 - \mathrm{i}\boldsymbol{k}\cdot\boldsymbol{x} + \frac{(-\mathrm{i}\boldsymbol{k}\cdot\boldsymbol{x})^2}{2} + o\big((\boldsymbol{k}\cdot\boldsymbol{x})^2\big)\Big) p_\delta(|\boldsymbol{x}|) d\boldsymbol{x}. \end{aligned} \tag{6}$$

As $p_\delta(|\boldsymbol{x}|)$ is an even function of $\boldsymbol{x}$, so

$$\int_{B_\delta(\boldsymbol{0})} \boldsymbol{k}\cdot\boldsymbol{x} p_\delta(|\boldsymbol{x}|) d\boldsymbol{x} = 0. \tag{7}$$

Furthermore, since $B_\delta(\boldsymbol{0})$ is compact, the assumption (2) ensures that the covariance matrix has finite entries. Using (7) in (6) we obtain

$$\hat{p}_\delta(\boldsymbol{k}) = \int_{B_\delta(\boldsymbol{0})} p_\delta(|\boldsymbol{x}|) d\boldsymbol{x} - \boldsymbol{k}^\top \boldsymbol{K}\boldsymbol{k} + o\big(\boldsymbol{k}^\top \boldsymbol{K}\boldsymbol{k}\big). \tag{8}$$

Substitute Eq. (8) into Eq. (5) to express the Fourier transform $\hat{G}(t,\boldsymbol{k})$ of $G(t,\boldsymbol{x})$ as follows

$$\hat{G}(t,\boldsymbol{k}) = -\boldsymbol{k}^\top \boldsymbol{K}\boldsymbol{k}\hat{u}(t,\boldsymbol{k}) + o\big(\boldsymbol{k}^\top \boldsymbol{K}\boldsymbol{k}\big)\hat{u}(t,\boldsymbol{k}). \tag{9}$$

Take the Fourier transform of the nonlocal diffusion model (1) and apply Eq. (9) to obtain

$$\frac{\partial \hat{u}}{\partial t} = -\boldsymbol{k}^\top \boldsymbol{K}\boldsymbol{k}\hat{u}(t,\boldsymbol{k}) + o\left(\boldsymbol{k}^\top \boldsymbol{K}\boldsymbol{k}\right)\hat{u}(t,\boldsymbol{k}). \tag{10}$$

Again by looking at the lowest terms in (10) as $\boldsymbol{k} \to \boldsymbol{0}$, we obtain the diffusion limit satisfied by $\hat{u}(t,\boldsymbol{k})$ in the phase space [8,9]

$$\frac{\partial \hat{u}}{\partial t} = -\boldsymbol{k}^\top \boldsymbol{K}\boldsymbol{k}\hat{u}(t,\boldsymbol{k}) = (\mathrm{i}\boldsymbol{k})^\top \boldsymbol{K}(\mathrm{i}\boldsymbol{k})\hat{u}(t,\boldsymbol{k}). \tag{11}$$

Take the inverse Fourier transform of Eq. (11) to recover the governing Fickian diffusion equation presented in problem (3). □

3. Numerical investigation

In this section, we conduct numerical experiments to validate that the nonlocal diffusion model represented by Eq. (1) demonstrates Fickian diffusive tendencies asymptotically as $\boldsymbol{x}$ approaches $\pm\infty$. To achieve this, we assess the mean square displacement (MSD) concerning the solution u. It is widely recognized that Fickian diffusion, akin to microscopic Brownian motion, manifests as linear temporal variation [8,9]:

$$MSD(t) := \int_{\mathbb{R}^d} |\boldsymbol{x}|^2 u(t,\boldsymbol{x})d\boldsymbol{x} = Ct. \tag{12}$$

Specifically, when the $MSD(t)$ exhibits a linear relationship with time, the associated nonlocal diffusion model defined by Eq. (1) demonstrates Fickian diffusion behavior. Variations in the coefficient C denote distinct diffusion rates.

In the numerical experiments, we utilize the collocation method [7] to perform numerical experiments aimed at investigating the asymptotic behavior of solutions to the nonlocal diffusion model (1) in both one and two space dimensions. We consider both Gaussian and power-law kernels. Subsequently, we compare these solutions with those of the corresponding Fickian diffusion Eq. (3), employing a finite difference method for computation. This comparative analysis serves to validate the theoretical insights presented in Section 2.

Hence, in order to support the findings in Section 2, we compare the $MSD(t)$, defined in Eq. (12), for the solutions of the nonlocal diffusion model (1), employing both Gaussian and power-law kernels, and the Fickian diffusion Eq. (3) to ascertain whether they both exhibit linearity in time and so the Fickian diffusion or Brownian motion behavior.

3.1. Behavior of the one-dimensional nonlocal diffusion model

We perform numerical experiments for the one-dimensional nonlocal diffusion model (1), employing both Gaussian and power-law kernels in Examples 1 and 2, respectively, and the Fickian diffusion Eq. (3). We choose the following Gaussian with $D = 5\times 10^{-3}$ to numerically approximate a Dirac delta initial data located at the origin at the initial time $t = 0$

$$u_0(x) = \frac{1}{\sqrt{4\pi D}} \exp^{-\frac{x^2}{4D}} \qquad x \in \mathbb{R}.$$

Example 1 (*One-dimensional Gaussian Kernel*)**.** The kernel is defined as

$$p_\delta(|x|) := \begin{cases} \dfrac{4}{5^{\frac{7}{2}}} e^{-\frac{x^2}{2\sigma^2}} \left(\displaystyle\int_{-\delta}^{\delta} x^2 e^{-\frac{x^2}{2\sigma^2}} dx \right)^{-1} & x \in [-\delta,\delta], \\ 0 & \text{elsewhere.} \end{cases} \tag{13}$$

In this example simulation, we calculate solutions for the one-dimensional nonlocal diffusion model (1) with $\delta = 0.2$ and $\sigma = 0.02$ in (13). Subsequently, we compare these solutions with the solutions of the corresponding Fickian diffusion Eq. (3), where the diffusion coefficient $\boldsymbol{K}$ is determined by (4) which depends on the horizon δ. Finally, we compute the mean square displacement $MSD(t)$ for the solutions of the nonlocal diffusion model (1) and the Fickian diffusion Eq. (3). The numerical results are presented in Fig. 1.

We note a remarkable consistency between the solutions and the mean square displacement $MSD(t)$ of the nonlocal model (1) and those of the corresponding Fickian diffusion Eq. (3). Notably, the mean square displacement $MSD(t)$ of the nonlocal model exhibits a linear relationship with respect to time t, providing strong support for the theoretical findings.

Example 2 (*One-Dimensional Weakly Singular Power-Law Kernel*)**.** The kernel is defined as $p_\delta(|x|) = |x|^{-\sigma}$ for $x \in [-\delta,\delta]$ or 0 elsewhere. In this simulation example, we compute the solution for the one-dimensional nonlocal diffusion model (1) with $\sigma = 0.5$, and $\delta = 0.2$. The obtained solution is then compared with the solution of the corresponding Fickian diffusion Eq. (3), along with an analysis of their mean square displacement $MSD(t)$. The numerical outcomes are depicted in Fig. 2.

Once again, we observe a consistency between the solutions and their respective $MSD(t)$ profiles. It is noteworthy to mention a slight disparity between the solutions of the Fickian diffusion Eq. (3), specifically in the middle plot of the second row in Fig. 1 compared to the middle plot in Fig. 2. Despite employing the same horizon $\delta = 0.2$ in Eq. (4), different kernels $p_\delta(|x|)$ are utilized. The Gaussian kernel and the power-law kernel in (4) have different decaying rates, when truncated to the same domain $[x-\delta, x+\delta]$, generate solutions with subtle differences. In summary, these findings once again strongly support the theoretical underpinnings.

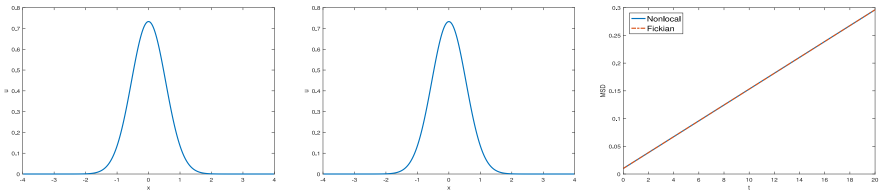

Fig. 1. Plots for Example 1: Left: The solution of the one-dimensional nonlocal diffusion model (1) with the Gaussian kernel specified in Example 1. Middle: The solution of the Fickian diffusion Eq. (3). Right: Mean square displacement $MSD(t)$ of both solutions.

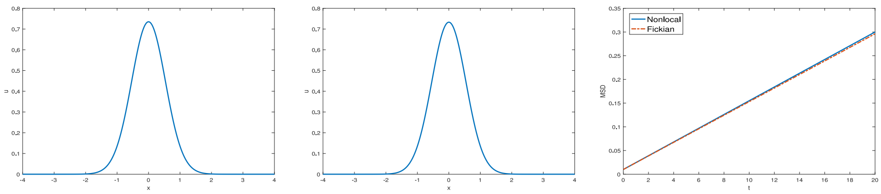

Fig. 2. Plots for Example 2: Left: The solution of the one-dimensional nonlocal diffusion model (1) with the weakly singular power-law kernel specified in Example 2 with $\sigma = 0.5$. Middle: The solution of the Fickian diffusion Eq. (3). Right: Mean square displacement $MSD(t)$ of both solutions.

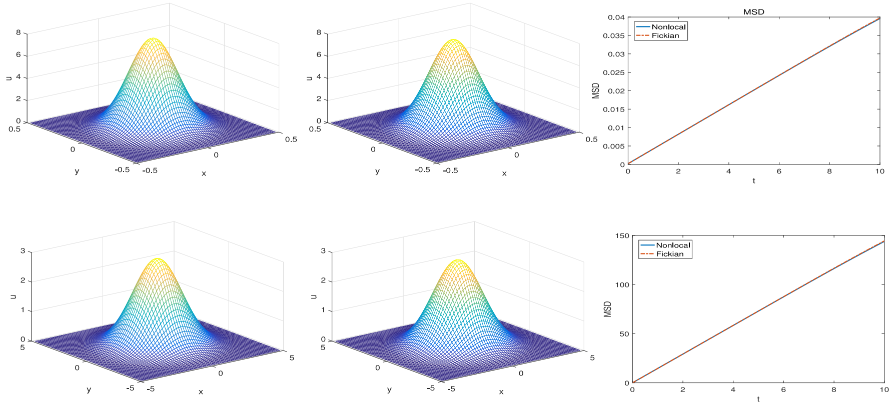

Fig. 3. Plots for Example 3: Left Column: Solutions of the two-dimensional nonlocal diffusion model (1) with the Gaussian kernel specified in Example 3. Middle Column: Solutions of the Fickian diffusion Eq. (3). Right Column: Mean square displacement $MSD(t)$ of their solutions. First Row: $\sigma = 0.02$ and $\delta = 0.1$. Second Row: $\sigma = 0.2$ and $\delta = 1$.

3.2. Behavior of the two-dimensional nonlocal diffusion model

We perform numerical experiments for the two-dimensional nonlocal diffusion model (1), employing both Gaussian and power-law kernels in Examples 3 and 4, respectively, and the Fickian diffusion Eq. (3). As a mollification of the Dirac delta initial condition located at the origin at the initial time $t = 0$, we use the following two-dimensional Gaussian pulse as initial data

$$u_0(\boldsymbol{x}) = \frac{1}{2\pi D} \exp^{-\frac{|\boldsymbol{x}|_2^2}{2D}} \qquad \boldsymbol{x} \in \mathbb{R}^2. \tag{14}$$

Here $|\cdot|_2$ refers to the Euclidean norm in $\mathbb{R}^2$.

Example 3 (*Two-dimensional Gaussian Kernel*)**.** The kernel is defined as:

$$p_\delta(|\boldsymbol{x}|) := \begin{cases} \dfrac{5}{2\pi\sigma^2} e^{-\frac{|\boldsymbol{x}|_2^2}{2\sigma^2}} & |\boldsymbol{x}|_2 \le \delta, \\ 0 & \text{elsewhere.} \end{cases} \tag{15}$$

In this simulation example, we investigate solutions for the two-dimensional nonlocal diffusion model given by Eq. (1). We consider two sets of parameters: $\sigma = 0.02$, $\delta = 0.1$, and $\sigma = 0.2$, $\delta = 1$ in (1) and (15). We select the neighborhood $B_\delta(\boldsymbol{x})$ as a closed disk centered at $\boldsymbol{x}$. The parameter $D = 10^{-4}$ is chosen in the initial data (14). Subsequently, we compare these solutions with those of the corresponding Fickian diffusion Eq. (3), where the diffusion tensor $\boldsymbol{K}$ is determined by (4) and depends on the horizon δ.

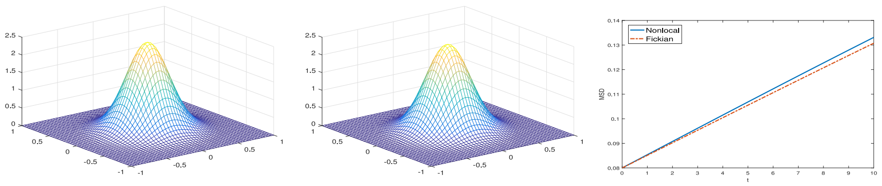

Fig. 4. Plots for Example 4: Left: The solution of the two-dimensional nonlocal diffusion model (1) with the weakly singular kernel specified in Example 4. Middle: The solution of the Fickian diffusion Eq. (3). Right: Mean square displacement $MSD(t)$ of both solutions.

We compute the mean square displacement $MSD(t)$ for the solutions of the nonlocal diffusion model (1) and the Fickian diffusion Eq. (3) with $\delta = 0.1$ and 1, respectively.

Note that due to the page limitation of the manuscript, this set of examples represents the *only* instance where two different horizon values of $\delta = 0.1$ and 1 are considered. Nonetheless, the numerical results presented in Fig. 3 provide a representative performance. These results again show a remarkable consistency between the solutions and the mean square displacement $MSD(t)$ of the nonlocal model (1) and those of the corresponding Fickian diffusion Eq. (3), and offer substantial support for the theoretical analysis.

Example 4 (*Two-dimensional Weakly Singular Kernel*)**.** The two-dimensional weakly singular kernel is chosen in the separable form:

$$p_\delta(|\boldsymbol{x}|) := \begin{cases} \dfrac{1}{|x_1|^{1/2}} \dfrac{1}{|x_2|^{1/2}} & |\boldsymbol{x}|_\infty \le \delta, \\ 0 & \text{elsewhere.} \end{cases} \tag{16}$$

For simulation simplicity, we define the neighborhood $B_\delta(\boldsymbol{x})$ as a closed square parallel to the coordinate axes, with a side length of 2δ, centered at $\boldsymbol{x}$. It is a closed "ball" in the $|\cdot|_\infty$ norm with a radius of $\delta = 0.2$ as specified in (16).

$D = 10^{-4}$ is chosen in (14). The solution for the two-dimensional nonlocal diffusion model (1) is computed with $\delta = 0.2$, and is compared with the solution of the Fickian diffusion Eq. (3). Additionally, we compute the mean square displacement $MSD(t)$ for both the solutions of the nonlocal diffusion model (1) and the Fickian diffusion Eq. (3) with the same $\delta = 0.2$.

The numerical findings depicted in Fig. 4 illustrate the close agreement between the solutions of the nonlocal diffusion model (1) and of the Fickian diffusion Eq. (3). We note a subtle discrepancy between the slope of the $MSD(t)$ for the Fickian diffusion equation and the nonlocal diffusion model. Note that the $MSD(t)$ for both solutions demonstrates a linear correlation with time t, indicative of Fickian diffusion or Brownian motion. The slight discrepancy between the slopes of the $MSD(t)$ for the two models indicates slightly different diffusion rates, which is expected to be attributed, in part, to the numerical errors due to the relatively large jump of the kernel $p_\delta(|\boldsymbol{x}|)$ across the boundary $\partial B_\delta(\boldsymbol{x})$ and its lack of rotational invariance. This analysis underscores the intricate dynamics captured by both models and highlights the nuanced influence of the chosen kernel function on their respective behaviors.

Data availability

No data was used for the research described in the article.

Acknowledgments

This work was funded in part by the National Natural Science Foundation of China under Grant 12001337 and by the National Science Foundation, USA under Grants DMS-2012291 and DMS-2245097. All data generated or analyzed during this study are included in this article.

References

[1] M. D'Eli, Q. Du, M. Gunzburger, R. Lehoucq, Nonlocal convection–diffusion problems on bounded domains and finite-range jump processes, Comput. Methods Appl. Math. 17 (2017) 707–722.
[2] Q. Du, M. Gunzburger, R. Lehoucq, K. Zhou, A nonlocal vector calculus, nonlocal volume-constrained problems, and nonlocal balance laws, Math. Models Methods Appl. Sci. 23 (2013) 493–540.
[3] M. Yang, D.B. Del-castillo negrete, G. Zhang, Y. Cao, A probabilistic scheme for semilinear nonlocal diffusion equations with volume constraints, SIAM Numer. Anal. 61 (2023) 2718–2743.
[4] K. Diethelm, The Analysis of Fractional Differential Equations, in: Ser. Lecture Notes in Mathematics, vol. 2004, Springer-Verlag, Berlin, 2010.
[5] V.J. Ervin, J.P. Roop, Variational solution of fractional advection dispersion equations on bounded domains in $\mathbb{R}^d$, Numer. Methods Partial Differential Equations 23 (2007) 256–281.
[6] I. Podlubny, Fractional Differential Equations, Academic Press, 1999.
[7] H. Wang, H. Tian, A fast and faithful collocation method with efficient matrix assembly for a two dimensional nonlocal diffusion model, Comput. Methods Appl. Mech. Engrg. 273C (2014) 19–36.
[8] M.M. Meerschaert, A. Sikorskii, Stochastic Models for Fractional Calculus, De Gruyter, 2019.
[9] R. Metzler, J. Klafter, The random walk's guide to anomalous diffusion: A fractional dynamics approach, Phys. Rep. 339 (2000) 1–77.